Universitatea Babeș-Bolyai, Facultatea de Fizică, Cluj-Napoca

Study of luminescence dosimetric properties of glass and vitroceramic systems composed of yttrium, aluminum, silicon, boron, phosphorus and gadolinium oxides

Ph.D. thesis summary

Andrada-Roxana Paşcu

Promoter: Prof. Dr. Viorica Simon

Cluj-Napoca 2019

The research discussed in the present thesis was carried out at the Environmental Radioactivity and Nuclear Dating Centre within the Interdisciplinary Research Institute on Bio-Nano-Science of the Babeş-Bolyai University in Cluj-Napoca, Romania.

Andrada-Roxana Paşcu benefited from financial support from:

The Romanian National Authority for Scientific Research CNCS-UEFISCDI through project PN-II-RU-TE-2014-4-1009.

The Sectorial Operational Programme for Human Resources Development 2007-2013, co-financed by the European Social Fund, under the project number POSDRU/187/1.5/S/155383 with the title "Quality, excellence, transnational mobility in doctoral research".

Contents

Keywords: *luminescence dosimetry, ionizing radiation, thermoluminescence, optically stimulated luminescence, glass system, glass-ceramic (vitroceramic) system, dosimeter*

Introduction

Radiation dosimetry with solid luminescent materials is a well-established method of monitoring ionizing radiation (Bos, 2001). Luminescent materials are crystalline solids able to store part of the ionizing radiation energy in the form of trapped charge that upon stimulation with heat or light can result in a luminescence signal. If heat is used to release the trapped charge, the light emission is called thermoluminescence (TL) and if the trapped charge is released by exposure to light, the light emission is called optically stimulated luminescence (OSL). The amount of trapped charge within a luminescent material is proportional to the absorbed dose of ionizing radiation.

Nowadays, there is a constant need for new materials specifically tailored to meet the growing demands of medical, industrial, agricultural and space applications based on the use of ultraviolet, X-rays, high-energy particles (alpha particles, protons, charged ions, fast neutrons), beta and gamma radiations.

Development of technologies employing high-dose irradiation to modify the properties of various materials, sterilize medical products, disinfect agricultural products, control the potential defects in large machine parts and equipment has revealed the very limited number of luminescent materials able to accurately measure medium and high-doses of ionizing radiation (Kortov, 2014). High-dose detectors are also needed for radiation monitoring of nuclear power station equipment and storages of spent nuclear fuel (Kortov, 2014). Taking into account that the current methods, e.g. electron spin resonance (ESR), optical absorption (OA), calorimetry and chemical reactions in irradiated solutions, used for high-dose measurements employ detectors which have rather narrow useful dose range and not high measurement accuracy, a high-dose luminescent detector development is an imperative necessity (Kortov and Ustyantsev, 2013). In order to keep the luminescent and dosimetric characteristics stable under high exposure doses, it is important to select radiation resistant materials. It was found that structural disordered compounds and low-dimensional materials (glasses, ceramics, vitroceramics) show high radiation resistance. Moreover, it has been shown that radiation-resistant aluminum and yttrium oxides contained in orthoaluminate ($YAlO_3$) crystals allow making detectors capable of measuring doses up to 5-10 kGy (Kortov, 2014).

Moreover, there is still increasing interest for finding luminescent dosimeters that can be used in the rapidly growing medical field for point measurements, dose profile measurements, two-dimensional (2D) dose mapping (especially, in quality assurance and dose verification in radiotherapy) (Yukihara et al., 2016), and real-time in-vivo OSL dosimetry. In

radiotherapy, precise measurements of doses ranging between 0.1 and 200 Gy, employing ~2 Gy dose fractions, are required (Akselrod et al., 2007). Also, 2D dosimetry with high spatial resolution is needed for modalities where steep gradients of dose distributions occur, such as is the case in intensity modulated radiotherapy, which enable highly conformal treatment plans with reduced absorbed dose to healthy tissues. The real-time in-vivo dosimetry system consists of a luminescent crystal attached to an optical fibre cable, used both for transmitting the stimulation light and the emitted OSL signal (Olko, 2010). It can be placed on the body at points of interest to perform entrance and exit dose measurements or, because of the very low diameter of the cable (2 mm), introduced to the body for intracavitary dose measurements.

Neutron dosimetry is also limited by the insufficient number of luminescent materials. Neutron detection relies on secondary charged particles and photons created by neutron interaction with the detector itself or surrounding material. Elastic neutron scattering with hydrogen nuclei create recoil protons with energies comparable to the incident neutrons, whereas nuclear capture reactions generate various types of charged particles with energies of a few MeV, gamma rays, and conversion electrons. These secondary resulting radiation deposit energies in the detector giving rise to a neutron induced signal (Yukihara et al., 2008).

The aim of this study is to explore the thermally and optically stimulated luminescent properties of various glass and vitroceramic systems composed of yttrium, aluminum, silicon, boron, phosphorus and gadolinium oxides in order to assess the suitability of their use as radiation dosimeters for high-dose, medical and neutron dosimetry.

This thesis is structured in 3 main chapters. Chapter 1 contains some of the results published in the article I authored (Pascu et al., 2017). Chapter 3 relies mainly on unpublished results, as well as on articles I authored (Pascu et al., 2017) and co-authored (Biró et al., 2015; Kadari et al., 2016). The outline of the thesis is as follows:

Chapter 1 introduces the basic concepts in thermoluminescence (TL) and optically stimulated luminescence (OSL) dosimetry. The principles and mechanism of TL and OSL production are described via band model and general equations governing the luminescence process. The general characteristics of TL and OSL materials assessed in this work and methods of thermal and structural analysis are also presented.

Chapter 2 composes of literature study and presents the current status of materials used for TL and OSL dosimetry. The first part offers a review of compounds specifically manufactured for luminescence dosimetry purposes, including commercially available TL and OSL dosimeters, glass systems, polycrystalline ceramics and glass-ceramics (vitroceramics).

The second part describes some of the unconventional materials used for luminescence retrospective dosimetry.

Chapter 3 presents TL and OSL dosimetry investigations of glass and vitroceramic systems composed of yttrium, aluminum, silicon, boron, phosphorus and gadolinium oxides. The basic dosimetric properties, such as sensitivity to ionizing radiation, dose response, minimum detectable dose (MDD), repeatability of response following multiple measurement cycles, batch homogeneity, stability of the luminescent signal in time (fading), energy response (Z_{eff}) and optical bleaching (sensitivity to light) are studied. For the compound showing the best dosimetric characteristics, modeling of the thermoluminescence mechanism, simulation of the glow curve and determination of kinetic parameters are performed.

At the end of the thesis **conclusions** are being summarized and a rating scale of 1 (low) to 5 (high) is employed to rate the TL dosimetric potential of each material.

1. Basic concepts in thermoluminescence (TL) and optically stimulated luminescence (OSL) dosimetry

Luminescence is the term describing the emission of light from a material as a result of its atomic and molecular excitation. This emission, which does not include black body radiation, represents the release of energy stored within the material through various types of excitation of the electronic system of the material (Furetta and Weng, 1998).

Fig 1.1. shows a simplified energy diagram for luminescence processes comprising of crystal irradiation, storage of radiation energy within the crystal lattice at point defects and crystal stimulation with heat or light. It is based on the General One-Trap (GOT) model, which includes a single type of electron trap *T* and a single type of radiative recombination centre *L*. During the interaction of ionizing radiation with a luminescent material, the electrons receive sufficient energy to make the transition from the valence band to the conduction band, leaving behind an unsatisfied bond, seen as positive charge and defined as a hole. Thus, with every promoted electron from the valence band to the conduction band, an electron-hole pair is created. Holes can migrate within the valence band until they get trapped at defects with negative charge and function as recombination centres *L*. As the concentration of electrons in the conduction band has to be quasistationary, electrons will either return to the valence band or become trapped at defects *T* within the band gap. The small part of trapped electrons will remain stored within defects a period of time equal with the depth of the trap *E*, which represents the difference in energy between the bottom of the conduction band and the localized

level. A trap is considered to be of interest in dosimetry if the probability of thermal eviction (without external stimulation) of the electrons is negligible. By stimulating the luminescent material either thermally (TL) or optically (OSL), trapped electrons gain sufficient energy to overcome the potential barrier of the trap and are released into the conduction band. In the attempt of electrons to return from the conduction band to the valence band, a fraction of the electrons will get retrapped, while the rest will recombine with the trapped holes at the recombination centres *L*. If the recombination centre is radiative, it will result in a photon emission. The total emitted TL or OSL associated with a particular trapping level is proportional to the trapped charge concentration and, in the ideal case, to the radiation dose absorbed by the luminescent material.

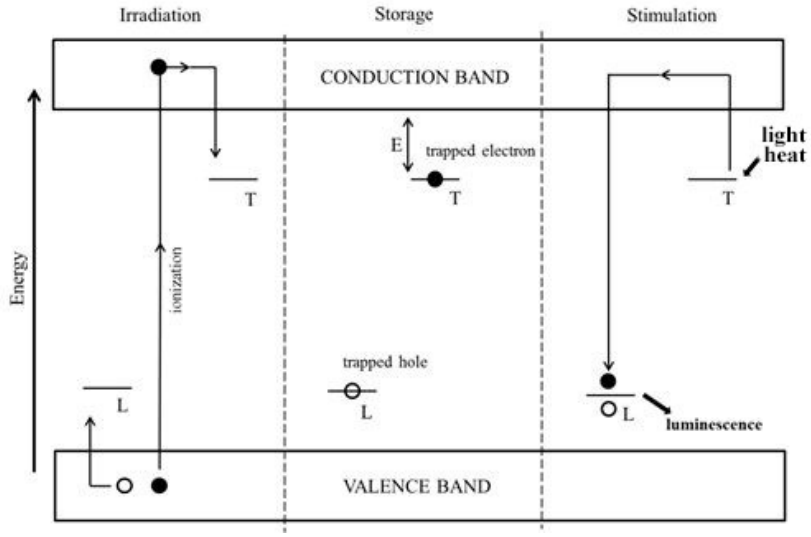

Fig. 1.2. Simplified band model illustrating TL and OSL processes, based on the one trap-one recombination centre model. Solid circles are electrons, open circles are holes. Level T represents an electron trap centre placed at depth E below the conduction band and level L represents a recombination centre. Adopted from Aitken (1998).

2. Current status of materials developed for thermoluminescence (TL) and optically stimulated (OSL) dosimetry

The first use of luminescent materials in ionizing radiation dosimetry is attributed to Daniels et al. during the late 1940s. These investigations were continued by John Cameron and led to the development of LiF as thermoluminescence dosimeter (Pradhan et al., 2008). The credit for the discovery of OSL in radiation dosimetry should go to Albrecht and Mandeville in the mid-1950s, who demonstrated that X-ray-exposed BeO samples exhibited an ultraviolet emission following a photo-stimulation by a light of wavelength 410 nm (Pradhan et al., 2008).

Antonov-Romanovskii et al., Bräunlich et al., and Sanborn and Beard have undergone the first experiments with all-optical luminescence measurements for dosimetry purposes (Akselrod et al., 2007). These initial studies focused on sulphide dosimetry materials as well as on materials originally tailored for thermoluminescence dosimetry (Ce-, Sm-, and Eu-doped MgS, CaS and SrS) (McKeever and Moscovitch, 2003; Pradhan et al., 2008).

Since then an impressive number of materials have been developed and studied in order to be applied in various radiation dosimetry fields including personnel and environmental monitoring, medical dosimetry, retrospective and accident dosimetry, high-dose dosimetry, space dosimetry, neutron dosimetry and high-energy charged particle (HCP) dosimetry. Although TL and OSL phenomenon can be observed in many materials, only some of them fulfill the requirements for dosimetry.

In general, the dosimetry applications can be grouped into four classes: personnel, environmental, medical (radiotherapy and diagnostic radiology) and radiation processing (sterilization, food processing, material testing) (Bos, 2001; Soares, 2002). **Table 2.1** presents the demands and constraints of each dosimetric area to be met by a luminescent dosimeter.

Table 2.1. Dosimetric requirements in some major application fields (Bos, 2001; Soares, 2002).

Application	Dose range (Gy)	Uncertainty 1 S.D. (%)	Tissue equivalency	Radiation type				
				High-E γ	Low-E γ	ß	ē	n
Personnel	$10^{-5} – 10^{-1}$	-30, +50	+	+	+	+	+	+
Environmental	$10^{-6} – 10^{-2}$	±30	-	+	+	+	-	+
Medical								
Radiotherapy	$10^{-1} – 10^{2}$	±3.5	+	+	+	+	+	+
Radiodiagnosis	$10^{-6} – 10$	±3.5	+					
Radiation processing	$10^{2} – 10^{7}$	±15	-	+	-	-	+	-

The ideal luminescent material should satisfy the following properties in order to be suitable for dosimetric purposes (McKeever et al., 1995; Akselrod et al., 2007; Kortov, 2007; Azorin, 2014; Yukihara et al., 2014):

- high sensitivity (high signal output per unit absorbed dose),
- wide interval in which the dose response relationship is linear,
- low fading (high stability of the signal in time given by deep thermally stable traps),
- independence of the energy of the incident radiation,

- resistance to environmental factors (mechanically strong, chemically inert, and radiation resistant),
- the luminescence spectrum should correspond to the maximum spectral sensitivity of the photomultiplier,
- simple TL glow curve (with one isolated peak), in the case of TL materials,
- trapping centers whose trapped charges can be easily optically stimulated (i.e. high photoionization cross-section) using light sources with wavelengths well separated from the emission bands of the recombination centers, in the case of OSL materials.

Despite of the great number of identified materials showing TL and OSL signals, only a few of them present adequate dosimetric properties and are commercially available. While thermoluminescence dosimetry benefits from a wide range of dosimeters and instruments based on crystalline and glass materials like LiF:Mg,Ti, CaF:Mn, CaSO4:Dy, $Li_2B_4O_7$, alumophosphate glasses and others (Akselrod et al., 2007), optically stimulated luminescence dosimetry relies only on two, Al_2O_3:C and BeO (Yukihara et al., 2013).

The successful developments as well as the limitations (e.g. the decrease in the response of high sensitive LiF:Mg,Cu,P and Al_2O_3:C with increasing ionization density of the radiation field, signal saturation at high doses, fading etc.) of commercial TL and OSL dosimeters have been taken into account for establishing some general requirements for the development and/or selection of newly and highly efficient dosimetric materials (Kortov, 2007; Olko, 2010).

As such, many studies have searched for new TL and OSL materials with suitable dosimetric properties. However, these materials have not been accepted for dosimetry probably because most of them showed one or more undesirable features such as fading, low sensitivity to radiation, high effective atomic number, or even self-dose (Oliveira et al., 2016).

The real advantage of some of these materials in comparison with others is simply in the optimal combination of thermal and optical energy depths of the traps, in fine separation between the emission and stimulation bands, and in a high photoionization cross-section of the traps (Akselrod et al., 2007).

3. Luminescence study of compounds based on yttrium, aluminum, silicon, boron and phosphorus oxides

The potential of vitroceramic and glass systems based on yttrium, aluminum, silicon, boron and phosphorus oxides for radiation dosimetry applications using thermoluminescence and optically stimulated luminescence techniques was investigated.

Silicate glasses, glass-ceramics (vitroceramics) and ceramics efficiently fulfill the role of luminescent hosts due to their rigid and very stable crystal structures. Moreover, the luminescent materials based on silicates as host material are characterized by strong chemical stability, high-energy ion irradiation resistance, as well as high UV and visible light transmittance (Barve et al., 2015). Incorporating rare-earth ions as dopants into the host lattice may led to a better stability of the compound and/or enhance the sensitivity to ionizing radiation of the luminescent materials (Laopaiboon and Bootjomchai, 2015; Alajerami et al., 2013).

Borosilicate glasses are characterized by four types of traps: network microstructure defect (E'-defect), non-bridging oxygen hole centers, multivalent ion centers, and network modifier defects (Clark et al., 2013). The dissolution mechanism of gadolinium in borosilicate glasses revealed that gadolinium first partitions to the borate-rich environment in the form of Gd-metalborate-like structure at low Gd_2O_3 concentrations and then to the silicate-rich environments causing the breaking of Si-O-Si bonds and the forming of non-bridging oxygen at high Gd_2O_3 concentrations (Li et al., 2001).

Yttrium aluminosilicate glasses are used as vectors for radiotherapy. Microspheres of Y_2O_3-Al_2O_3-SiO_2 (YAS) glasses, which contain ^{89}Y that can be transformed by neutron activation into the β-emitter ^{90}Y, are currently used in noninvasive cancer treatment, especially to treat liver cancer in humans, where their chemical durability is of prime importance. The most chemically durable YAS glass proved to be of $17Y_2O_3$-$19Al_2O_3$-$64SiO_2$ (mol%) composition (Erbe and Day, 1993). The radioisotope ^{90}Y has a half-life of 64.1 h. After the decay of ^{90}Y radioisotopes, the non-radiative and non-toxic microspheres continue to reside for a time in the targeted tissue.

Phosphate glasses are often used as biomaterials due to their chemical similarity to the natural bone. However, simple phosphate glasses are chemically unstable and require the addition of metal oxides to improve their chemical durability for various applications. Recently, neutron activated phosphate glasses microspheres with high Y_2O_3 content have also been used for brachytherapy applications. It has been demonstrated that adding Y_2O_3 to the

glasses structure improves its stability and durability (Biró et al., 2018; Christie et al., 2011; Fu and Christie, 2017).

Glass-ceramics are partially crystallized glasses that are produced by heating the glass-parent above its crystallization temperature. Thus, vitroceramics are solid polycrystalline compounds formed as a result of a controlled glass crystallization and contain one or more crystalline phases embedded in a residual glassy phase. In the crystallization process, nucleation and the uniform growth of small sized crystals (< 1μm) are of paramount importance. Glass nucleation takes place at considerably lower temperatures than the corresponding melting point and needs the presence of nucleation centers such as Cu, Ag, Au, or titan oxides, zirconium and phosphor. Generally, for this type of materials the crystallization achieved is above 90% and the crystals sizes range between 0.1 and 1 μm (Park and Lakes, 2007). Controlled crystallization yields strong, dense materials with inherent advantages over the conventional glass and ceramic compounds, such as significantly small or even negative thermal expansion coefficient, improved properties under mechanical stress and high radiation resistance (Park, 1984).

The vitroceramic sample with $40SiO_2 \cdot 59.5B_2O_3 : 0.5Gd_2O_3$ mol% nominal composition, was prepared by melting mechanically homogenized mixtures of H_3BO_3, SiO_2 and Gd_2O_3 analytical reagents of pro analysis purity at 1400°C for 15 minutes followed by fast undercooling to room temperature. The value chosen for the ratio between SiO_2 and B_2O_3 aimed to reduce the phase separation tendency governing the binary SiO_2-B_2O_3 glass system in the silica rich composition range (Polyakova, 2000; Plodinec, 2000).

The highly-homogenized mixtures of Y_2O_3, Al_2O_3, SiO_2 and Gd_2O_3 pure reagents (pro analysis purity) were melted at 1550°C for 30 minutes in a Carbolite furnace and thereafter quickly cooled to room temperature. Samples having the $(17\text{-}x)Y_2O_3 \cdot 19Al_2O_3 \cdot 64SiO_2 : xGd_2O_3$ mol% nominal composition, where $0 \leq x \leq 15$ mol% Gd_2O_3, were obtained in vitreous phase, while the 0.2 mol% and 10 mol% Gd_2O_3 doped binary (Y_2O_3-Gd_2O_3, Al_2O_3-Gd_2O_3, SiO_2-Gd_2O_3) and ternary (Y_2O_3-Al_2O_3-Gd_2O_3, Y_2O_3-SiO_2-Gd_2O_3, Al_2O_3-SiO_2-Gd_2O_3) systems were obtained in vitroceramic phase.

The vitroceramic sample with $30P_2O_5 \cdot 40SiO_2 : 30Y_2O_3$ mol% nominal composition was prepared by melting mechanically homogenized mixtures of Y_2O_3, $NH_4H_2PO_4$ and SiO_2 analytical reagents of pro analysis purity at temperatures between 1400°C and 1500°C for 30 minutes followed by fast undercooling at room temperature.

Table 3.1 encompasses the prepared vitroceramics and glasses along with their effective atomic number (Z_{eff}) determined by using the Mayneord equation (Mayneord, 1937).

Most compounds have high Z_{eff} values, while $22.8Al_2O_3 \cdot 77SiO_2:0.2Gd_2O_3$ and $99.8Al_2O_3:0.2Gd_2O_3$ have similar values with that of compact bone, $Z_{eff} = 13.59$ (Bos, 2001).

Table 3.1. List of materials and their effective atomic number

Nr. crt	Sample	Z_{eff}
1	$99.8Y_2O_3:0.2Gd_2O_3$	35.77
2	$99.8Al_2O_3:0.2Gd_2O_3$	13.77
3	$99.8SiO_2:0.2Gd_2O_3$	15.32
4	$46.8Y_2O_3 \cdot 53Al_2O_3:0.2Gd_2O_3$	31.12
5	$20.8Y_2O_3 \cdot 79SiO_2:0.2Gd_2O_3$	28.52
6	$22.8Al_2O_3 \cdot 77SiO_2:0.2Gd_2O_3$	14.84
7	$90Y_2O_3:10Gd_2O_3$	41.16
8	$90Al_2O_3:10Gd_2O_3$	38.07
9	$90SiO_2:10Gd_2O_3$	42.86
10	$24.2Y_2O_3 \cdot 65.8Al_2O_3:10Gd_2O_3$	39.34
11	$8.9Y_2O_3 \cdot 81.1SiO_2:10Gd_2O_3$	42.50
12	$20.6Al_2O_3 \cdot 69.4SiO_2:10Gd_2O_3$	41.54
13	$17Y_2O_3 \cdot 19Al_2O_3:64SiO_2$	26.06
14	$16.8Y_2O_3 \cdot 19Al_2O_3 \cdot 64SiO_2:0.2Gd_2O_3$	26.62
15	$14Y_2O_3 \cdot 19Al_2O_3 \cdot 64SiO_2:3Gd_2O_3$	32.66
16	$12Y_2O_3 \cdot 19Al_2O_3 \cdot 64SiO_2:5Gd_2O_3$	35.76
17	$7Y_2O_3 \cdot 19Al_2O_3 \cdot 64SiO_2:10Gd_2O_3$	41.48
18	$2Y_2O_3 \cdot 19Al_2O_3 \cdot 64SiO_2:15Gd_2O_3$	45.59
19	$40SiO_2 \cdot 59.5B_2O_3: 0.5Gd_2O_3$	17.70
20	$30P_2O_5 \cdot 40SiO_2: 30Y_2O_3$	28.18

Luminescence measurements were carried out using an automated Risø TL/OSL Luminescence Reader, model TL/OSL-DA-20, (Risø National Laboratory, Røskilde, Denmark). TL signals were recorded by ramp heating the samples to 500°C, using a constant heating rate of 5°C/s in nitrogen atmosphere. OSL signals were recorded during constant power (~36 mW/cm^2) stimulation using blue LEDs (470 nm, FWHM 20 nm) for 100 s at a temperature of 150°C (5°C/s heating rate). All luminescence emissions have been detected using a bi-alkali EMI 9235QA photomultiplier tube through a Hoya U-340 filter (transmission between 290-390 nm).

Samples were measured using tens of milligrams of powder in stainless steel cups to eliminate the variability of luminescence intensity due to the sample shape, mediated by light photon scattering at the interface of the medium (Yusoff et al., 2005) and to reduce uncertainties related to beta dose rate calibration for analysis involving the integrated $^{90}Sr/^{90}Y$ beta source. After measurements, all data was mass normalized for 10 mg of sample.

TL signals used for analyses were determined by integrating the TL intensity over a certain temperature region and subtracting the native signal of the unexposed sample for the selected temperature region of interest. For OSL analyses it was used the net OSL signal obtained by subtracting the OSL signal observed towards the end of the stimulation period from the earlier OSL signal. Thus, the OSL signals were integrated over the first 2 s of stimulation minus the background evaluated from the last 2 s and the corresponding native signal of the unexposed sample was afterwards deducted. Murray et al. (1997) demonstrated that the initial OSL signal intensity is directly proportional to the integrated OSL signal and Banarjee et al. (2000) showed that the smallest statistical uncertainty (for both weak and bright signals) in the net OSL signal is achieved using the first few seconds of the decay curve (Bøtter-Jensen et al., 2003). This procedure also ensures the removal of the contribution from the instrumental background (e.g. including PMT dark counts and filter break through contributions).

The vitroceramic and glass samples were irradiated individually and automatically in the luminescence reader using the integrated $^{90}Sr/^{90}Y$ beta source, delivering approximately 0.15 Gy/s (absorbed dose in quartz) or at room temperature in a homogeneously field using a ^{60}Co gamma source, delivering a 3 Gy/h dose rate.

The basic luminescence dosimetric properties, such as sensitivity to ionizing radiation, dose response, minimum detectable dose (MDD), repeatability of response following multiple measurement cycles, batch homogeneity, stability of the luminescent signal in time (fading) and optical bleaching (sensitivity to light) have been studied. Moreover, modeling of the thermoluminescence mechanism, simulation of the glow curve and determination of kinetic parameters have also been performed for the compound showing the best dosimetric characteristics.

The suitability of $40SiO_2 \cdot 49.5B_2O_3 : 0.5Gd_2O_3$ for thermoluminescent radiation dosimetry purposes was evaluated. The 0.5 mol% Gd_2O_3 doped borosilicate vitroceramic showed an intense TL signal following irradiation with 6 Gy, linear dependency upon dose in the 0.75 – 9 Gy dose interval, good repeatability of the response over 5 measurement cycles and a relatively small value of the MDD (Pascu et al., 2017). A major shortcoming of this material was the exhibited TL signal in the low-temperature region of the glow curve (~100°C), considering that glow peaks with a maximum intensity occurring at temperatures below 200°C are associated with signals generally unstable at room temperature, being prone to rapid fading in a short time period. Thus, $40SiO_2 \cdot 59.5B_2O_3 \cdot 0.5Gd_2O_3$ is not suitable for long time span dosimetry applications and was discharged from further studies.

In order to assess their dosimetric potential, TL and OSL studies were performed on the 0.2 mol% and 10 mol% Gd_2O_3 doped binary (Y_2O_3-Gd_2O_3, Al_2O_3-Gd_2O_3, SiO_2-Gd_2O_3) and ternary (Y_2O_3-Al_2O_3-Gd_2O_3, Y_2O_3-SiO_2-Gd_2O_3, Al_2O_3-SiO_2-Gd_2O_3) vitroceramic systems and on the $(17\text{-}x)Y_2O_3 \cdot 19Al_2O_3 \cdot 64SiO_2 : xGd_2O_3$ ($0 \leq x \leq 15$ mol%) glass system. TL analysis revealed that the majority of vitroceramics doped with 0.2 mol% showed intense TL signals in the dosimetric range of the glow curve (above 200°C), very good values of repeatability (excluding $99.8Y_2O_3$:$0.2Gd_2O_3$), as well as acceptable MDD and batch homogeneity values. Besides $20.8Y_2O_3 \cdot 79SiO_2$:$0.2Gd_2O_3$ and $99.8Y_2O_3$:$0.2Gd_2O_3$, all vitroceramics presented a linear dependency in the 0.7 – 1000 Gy dose range. Two days following irradiation the remained signal of $99.8Al_2O_3$:$0.2Gd_2O_3$ and $22.8Al_2O_3 \cdot 77SiO_2$:$0.2Gd_2O_3$ was 69% and 73% (main dosimetric peak), respectively, while the signal loss after 100 days of storage was greater than 50%. Vitroceramics doped with 10 mol% generally gave less intense dosimetric TL signals, showing one main dosimetric peak, and were characterized by good repeatability (excepting $90SiO_2$:$10Gd_2O_3$) and homogeneity (excluding $90Y_2O_3$:$10Gd_2O_3$) values. The MDD values were particularly very high for $90SiO_2$:$10Gd_2O_3$ and $8.9Y_2O_3 \cdot 81.1SiO_2$:$10Gd_2O_3$. Apart from $90Y_2O_3$:$10Gd_2O_3$ and $24.2Y_2O_3 \cdot 65.8Al_2O_3$:$10Gd_2O_3$, all vitroceramics exhibited linear dose dependency up to 1000 Gy. The investigated $24.2Y_2O_3 \cdot 65.8Al_2O_3$:$10Gd_2O_3$ vitroceramic showed the smallest value of the remained signal of 48% 2 days after irradiation and only 12% over 100 days of storage. All glasses were sensitive to ionizing radiation and showed strong TL signals in the dosimetric region of the glow curve (above 200°C). The undoped glass along with the 5 mol% and 10 mol% Gd_2O_3 doped glasses were characterized by a linear dose response up to 1000 Gy. As example, **Fig. 3.1.** shows a TL glow curve and a TL dose response curve of the investigated 10 mol% Gd_2O_3 doped glass. Moreover, most glasses were characterized by good repeatability and batch homogeneity, as well as relatively small MDD values, when considering the peak placed at ~250°C. The remained signal 2 days following irradiation for the 0.2 mol% and 10 mol% Gd_2O_3 doped glasses was of 68% and 76% for the main dosimetric peak of the 10 mol% doped glass, respectively, while the remained signal after 100 days of storage time was less than 50%.

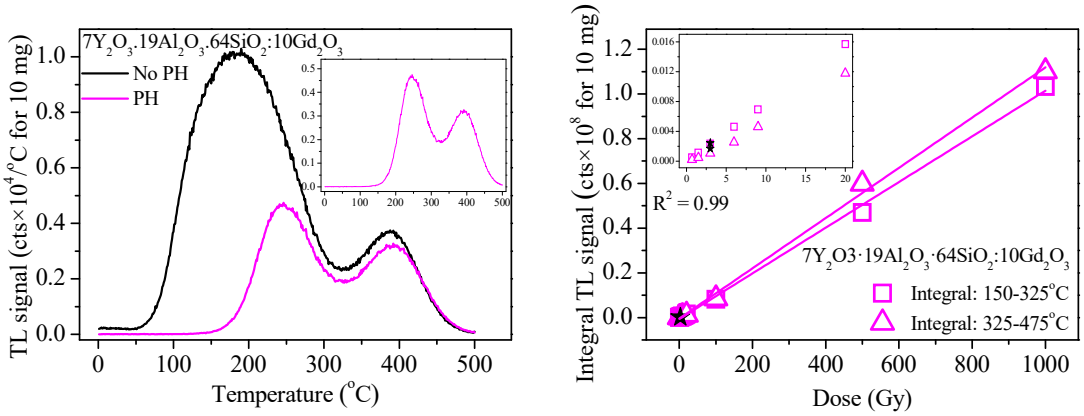

Fig 3.1. TL glow curve of $7Y_2O_3 \cdot 19Al_2O_3 \cdot 64SiO_2:10Gd_2O_3$ registered upon irradiation with a dose of 6 Gy, before (quoted - no PH) and after preheating (quoted - PH) the sample at 180°C for 10 s. For better visualization, the inset shows the decay curve of the preheated sample **(left)**. TL dose response of $7Y_2O_3 \cdot 19Al_2O_3 \cdot 64SiO_2:10Gd_2O_3$ measured in a single aliquot protocol over the 0.7-1000 Gy dose range and registered after preheating the sample at 180°C for 10 s. One aliquot was used. The selected region of interest is individually specified. The star symbols represent the repeat doses delivered to check for sensitivity changes. The inset graph shows the TL response over the 0.7-20 Gy dose interval **(right)**.

OSL investigations revealed that most Gd_2O_3 doped vitroceramics and glasses gave more intense OSL signals than their previously recorded TL signals following irradiation with 6 Gy. However, $90SiO_2:10Gd_2O_3$ and $8.9Y_2O_3 \cdot 81.1SiO_2:10Gd_2O_3$ did not exhibited bright OSL signals and were not further studied. Besides intense OSL signals, vitroceramics doped with 0.2 mol% Gd_2O_3 were characterized by satisfactory repeatability and homogeneity values, relatively small values of the MDD, while $99.8Y_2O_3:0.2Gd_2O_3$, $20.8Y_2O_3 \cdot 79SiO_2:0.2Gd_2O_3$ and $22.8Al_2O_3 \cdot 77SiO_2:0.2Gd_2O_3$ showed supralinear response in the 0.7 -1000 Gy dose range. Two days after irradiation, the OSL signal loss was 47% for $99.8Al_2O_3:0.2Gd_2O_3$ and 31% for $22.8Al_2O_3 \cdot 77SiO_2:0.2Gd_2O_3$. Over 100 days of storage, $99.8Al_2O_3:0.2Gd_2O_3$ showed a 35% additional reduction of the OSL signal, while $22.8Al_2O_3 \cdot 77SiO_2:0.2Gd_2O_3$ lost another 28%. Vitroceramics doped with 10 mol% generally exhibited higher values of repeatability, MDD and homogeneity, while $24.2Y_2O_3 \cdot 65.8Al_2O_3:10Gd_2O_3$ showed a supralinear dependence upon absorbed dose for the investigated 0.7-1000 Gy dose interval. Fading measurements were performed on the same vitroceramic and pointed out an extreme signal loss both 2 days and 100 days following irradiation. The sort-time fading was 61%, while for the long-time fading a value of 92% was registered. The Gd_2O_3 doped glasses showed bright OSL signals with one order of magnitude higher than the undoped glass. They were also characterized by very good

values of repeatability (except $16.8Y_2O_3 \cdot 19Al_2O_3 \cdot 64SiO_2:0.2Gd_2O_3$), MDD and homogeneity, and a linear dose dependency up to 1000 Gy (excluding the 0.2 mol% doped glass). **Fig. 3.2.** shows the OSL decay and dose response curves of the investigated 10 mol% Gd_2O_3 doped glass, while **Table 3.2** presents a summary of all OSL dosimetric properties of the Gd_2O_3 doped vitroceramics and glasses after preheating the samples at 180°C (5°C/s) for 10 s.

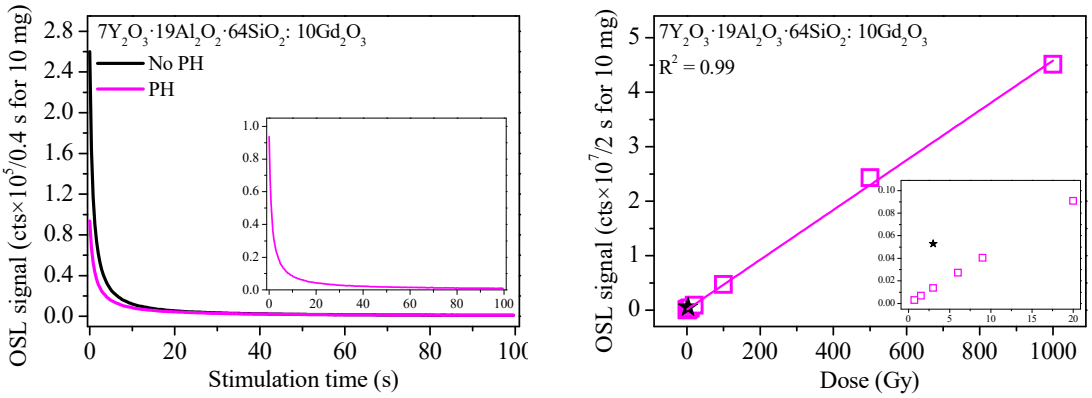

Fig. 3.2. OSL decay curve of $7Y_2O_3 \cdot 19Al_2O_3 \cdot 64SiO_2:10Gd_2O_3$ glass registered upon irradiation with a dose of 6 Gy, before (quoted - no PH) and after preheating (quoted - PH) the sample at 180°C for 10 s. For better visualization, the inset shows the decay curve of the preheated sample **(left)**. OSL dose response of $7Y_2O_3 \cdot 19Al_2O_3 \cdot 64SiO_2:10Gd_2O_3$ measured in a single aliquot protocol over the 0.7 – 1000 Gy dose range and registered after preheating the sample at 180°C for 10 s. One aliquot was used. The star symbols represent the repeat dose delivered to check for sensitivity changes. The inset graph shows the OSL response over the 0.7 – 20 Gy dose interval **(right)**.

The investigated glasses also suffered from significant fading. The 0.2 mol% doped glass showed a signal reduction of 34% 2 days after irradiation and 70% after 100 days of storage. The glass doped with 10 mol% exhibited a 34% signal loss after 2 days and 58% over 100 days. Optical bleaching of TL signals revealed that vitroceramics and glasses are very light sensitive, showing a significant reduction of the TL output. Moreover, all main dosimetric TL peaks shifted at higher temperatures, suggesting some traps are sensitive to optical stimulation, but the complexity of the glow curve generally remained unchanged.

Table 3.2. Summary of the OSL dosimetric properties of vitroceramics and glasses, after preheating the samples at 180°C (5°C/s) for 10 s.

Nr. crt.	Compound	Sensitivity [cts/2 s for 10 mg]	Linearity [Gy]	Repeatability [% dev from unity]	MDD [mGy]	Homogeneity [rel stdev %]	Signal loss [%]
1.	$99.8Y_2O_3$: $0.2Gd_2O_3$	1.4×10^5	0.7 – 200	0.4	11	10	-
2	$99.8Al_2O_3$:$0.2Gd_2O_3$	1.7×10^4	0.7 – 1000	16	55	12	82
3	$99.8SiO_2$:$0.2Gd_2O_3$	1.3×10^4	0.7 – 1000	4	31	15	-
4	$46.8Y_2O_3\cdot53Al_2O_3$:$0.2Gd_2O_3$	5.0×10^4	0.7 – 1000	13	41	13	-
5	$20.8Y_2O_3\cdot79SiO_2$:$0.2Gd_2O_3$	1.1×10^6	0.7 – 50	20	1	16	-
6	$22.8Al_2O_3\cdot77SiO_2$:$0.2Gd_2O_3$	6.0×10^5	0.7 – 200	11	1	12	59
7	$90Y_2O_3$:$10Gd_2O_3$	4.2×10^3	0.7 – 1000	64	284	11	-
8	$90Al_2O_3$:$10Gd_2O_3$	7.6×10^4	0.7 – 1000	5	15	10	-
9	$90SiO_2$:$10Gd_2O_3$	-	-	-	-	-	-
10	$24.2Y_2O_3\cdot65.8Al_2O_3$:$10Gd_2O_3$	3.1×10^4	0.7 – 500	7	21	14	92
11	$8.9Y_2O_3\cdot81.1SiO_2$:$10Gd_2O_3$	-	-	-	-	-	-
12	$20.6Al_2O_3\cdot69.4SiO_2$:$10Gd_2O_3$	1.5×10^3	0.7 – 1000	14	395	13	-
13	$17Y_2O_3\cdot19Al_2O_3\cdot64SiO_2$	1.1×10^4	0.7 – 1000	-	59	-	-
14	$16.8Y_2O_3\cdot19Al_2O_3\cdot64SiO_2$:$0.2Gd_2O_3$	1.3×10^5	0.7 – 500	16	4	3	70
15	$14Y_2O_3\cdot19Al_2O_3\cdot64SiO_2$:$3Gd_2O_3$	1.2×10^5	0.7 – 9[a]	5	12	6 [b]	-
16	$12Y_2O_3\cdot19Al_2O_3\cdot64SiO_2$:$5Gd_2O_3$	1.2×10^5	0.7 – 1000	5	9	10	-
17	$7Y_2O_3\cdot19Al_2O_3\cdot64SiO_2$:$10Gd_2O_3$	9.4×10^4	0.7 – 1000	5	7	9	58
18	$2Y_2O_3\cdot19Al_2O_3\cdot64SiO_2$:$15Gd_2O_3$	1.1×10^5	0.7 – 9[a]	5	-	8[b]	-

[a]*Was not tested for higher doses*
[b]*No preheating was applied*

Considering the previously reported results, most Gd_2O_3 doped vitroceramics and glasses could be successfully employed for high-dose dosimetry using both TL and OSL techniques. The wide range linearity of the investigated materials make them extremely attractive for measuring high-doses of ionizing radiation well above the saturation limit of 10 Gy, characteristic for the traditional TL materials (Furetta et al., 2001), and of 50 Gy and ~100 Gy for Al_2O_3:C and BeO OSLDs, respectively (Bøtter-Jensen et al., 2003; Sommer and Henniger, 2006). Taking into account the need for radiation-resistant materials that could keep the luminescent and dosimetric characteristics stable under high exposure doses (Kortov, 2014), the proven chemical durability of the $17Y_2O_3$-$19Al_2O_3$-$64SiO_2$ glass system (Erbe and Day, 1993) and the radiation-resistant aluminum and yttrium oxides contained in orthoaluminate ($YAlO_3$) crystals (Kortov, 2014) make these materials even more suitable candidates for luminescence high-dose dosimetry.

The Y_2O_3-Al_2O_3-SiO_2 glass system could also be used in medical dosimetry for radiotherapy measurements, which employ doses ranging between 0.1 and 200 Gy, with typical dose fractions of ~2 Gy (Akselrod et al., 2007). Moreover, the well-established biomedical applications of this glass system along with its strong OSL sensitivity to ionizing radiation, fast decay of the OSL signal, and high content of silicon oxide could extend the potential use of $(17\text{-}x)Y_2O_3 \cdot 19Al_2O_3 \cdot 64SiO_2 : xGd_2O_3$ glass system for real-time in-vivo OSL dosimetry, which enables real-time monitoring of the actual dose delivered to the patient. However, taking into account the lack of tissue equivalency of the materials, proper calibrations and energy corrections are required.

Radiation dosimetry relies on the possibility to assess the accrued dose by a luminescent material over variable time periods, depending on the requirements of the targeted dosimetry application. Thus, one of the most important dosimetric property is the signal stability in time. However, signal fading to different degrees over a variety of time scales is a common weakness of numerous newly developed TL and OSL materials. Besides the significant signal loss registered in the case of $24.2Y_2O_3 \cdot 65.8Al_2O_3$:$10Gd_2O_3$, TL and OSL short-time fading measurements of the Gd_2O_3 doped vitroceramics and glasses revealed that ~70% of the initial signal is recorded 2 days following irradiation. Taking into account that most dosimetric applications, including high-dose and medical dosimetry, benefit from a rapid evaluation of doses, plus the very good cycle-to cycle TL and OSL sensitivity exhibited by most materials, allow for realistic extrapolations of anomalous fading over the time scale of interest (Inrig et al., 2008). Thus, accurate measurements can be achieved by recording the luminescent signals in the first 2 days after irradiation and applying appropriate fading corrections.

The potential of $30P_2O_5 \cdot 40SiO_2:30Y_2O_3$ vitroceramic for thermoluminescent radiation dosimetry was also studied. The 30 mol% Y_2O_3 doped phosphosilicate was characterized by an intense TL signal placed in the dosimetric temperature range (~210°C and above), linear dependency in the 0.7-9 Gy dose interval, very good repeatability, a small MDD value, acceptable batch homogeneity and a signal loss of ~30% after 4 months of storage time (Biró et al., 2015). Considering $30P_2O_5 \cdot 40SiO_2:30Y_2O_3$ showed the best value in terms of signal fading, additional investigations were undertaken, such as thermoluminescence process modeling, determination of kinetic parameters and neutron sensitivity evaluation. The TTOR model successfully predicts the TL mechanism and the linear dependency upon dose exhibited by the sample, while the calculated values of the activation energy *E* and the frequency factor *s* for the main dosimetric peak were 1.27 eV and 4.78×10^{11} s^{-1}, respectively (Kadari et al., 2016). The preliminary investigations of the neutron sensitivity of $30P_2O_5 \cdot 40SiO_2:30Y_2O_3$ revealed a neutron energy dependent absorbed TL dose response (Biró et al., 2018). The previously reported results suggest that the 30 mol% Y_2O_3 doped phosphosilicate could be used for dose determinations in medical dosimetry, taking into account the exhibited linear TL response with dose in the range of fractionated teletherapy (0 to 2 Gy) and the TL response in mixed neutron-gamma fields.

A summary of the TL dosimetric properties of all investigated vitroceramics and glasses based on yttrium, aluminum, silicon, boron, phosphorus and gadolinium oxides is given in **Table 3.3**. In addition, a rating scale of 1 (low) to 5 (high) was employed to rate the dosimetric potential of each material based on its registered signal intensity, dose-range linearity, repeatability of response over multiple measurement cycles, minimum detectable dose, batch homogeneity and signal loss after 100 days of storage time.

Table 3.3. Summary of the TL dosimetric properties of all investigated glasses and vitroceramics, after preheating the samples at 180°C (5°C) for 10 s.

Nr. crt.	Compound	T [°C]	Sensitivity [cts/°C for 10 mg]	Linearity [Gy]	Repeatability [% scatter]	MDD [mGy]	Homogeneity [rel stdev %]	Signal loss [%]	Score
1.	$99.8Y_2O_3$: $0.2Gd_2O_3$	150-250	8.6×10^2	0.7 – 200	3	394	11	-	2
2	$99.8Al_2O_3$:$0.2Gd_2O_3$	150-400	8.5×10^3	0.7 – 1000	13	194	12	68	3
3	$99.8SiO_2$:$0.2Gd_2O_3$	250-450	1.2×10^3	0.7 – 1000	3	572	34	-	3
4	$46.8Y_2O_3\cdot53Al_2O_3$:$0.2Gd_2O_3$	150-400	6.4×10^2	0.7 – 1000	5	413	16	-	2
5	$20.8Y_2O_3\cdot79SiO_2$:$0.2Gd_2O_3$	150-300	7.4×10^4	0.7 – 500	5	5	10	-	4
		300-400	3.1×10^4		2	8	10		
6	$22.8Al_2O_3\cdot77SiO_2$:$0.2Gd_2O_3$	150-300	6.0×10^4	0.7 – 1000	5	24	12	54	4
		250-400	1.5×10^4		16	292	11	40	
7	$90Y_2O_3$:$10Gd_2O_3$	200-400	5.6×10^3	0.7 – 100	8	393	22	-	2
8	$90Al_2O_3$:$10Gd_2O_3$	150-350	2.3×10^4	0.7 – 1000	2	28	8	-	3
9	$90SiO_2$:$10Gd_2O_3$	200-400	2.6×10^2	0.7 – 1000	18	2642	9	-	1
10	$24.2Y_2O_3\cdot65.8Al_2O_3$:$10Gd_2O_3$	150-350	2.9×10^4	0.7 – 500	0.3	726	8	88	1
11	$8.9Y_2O_3\cdot81.1SiO_2$:$10Gd_2O_3$	250-450	3.3×10^2	0.7 – 1000	1	2322	10	-	2
12	$20.6Al_2O_3\cdot69.4SiO_2$:$10Gd_2O_3$	150-300	5.2×10^2	0.7 – 1000	4	166	8	-	3
13	$17Y_2O_3\cdot19Al_2O_3\cdot64SiO_2$	150-400	2.7×10^3	0.7 – 1000	-	183	-	-	3
14	$16.8Y_2O_3\cdot19Al_2O_3\cdot64SiO_2$:$0.2Gd_2O_3$	150-400	2.1×10^4	0.7 – 500	18	90	5	54	4
15	$14Y_2O_3\cdot19Al_2O_3\cdot64SiO_2$:$3Gd_2O_3$	150-325	8.2×10^3	0.7 – 9[a]	1	54	11[b]	-	3
		325-475	1.5×10^3		26	96	10[b]		
16	$12Y_2O_3\cdot19Al_2O_3\cdot64SiO_2$:$5Gd_2O_3$	150-325	6.6×10^3	0.7 – 1000	2	41	7	-	4
		325-475	2.5×10^3		72	83	13		
17	$7Y_2O_3\cdot19Al_2O_3\cdot64SiO_2$:$10Gd_2O_3$	150-325	4.7×10^3	0.7 – 1000	2	19	10	64	5
		325-475	3.3×10^3		55	74	10	45	
18	$2Y_2O_3\cdot19Al_2O_3\cdot64SiO_2$:$15Gd_2O_3$	175-300	4.9×10^3	0.7 – 9[a]	2	-	8[b]	-	3
		325-475	7.6×10^3		35		10[b]		
19	$40SiO_2\cdot59.5B_2O_3$:$0.5Gd_2O_3$[b]	60-300	1.0×10^4	0.75 – 9[a]	7	34	-	-	1
20	$30P_2O_5\cdot40SiO_2$:$30Y_2O_3$[c]	150-300	3.3×10^4	0.75 – 9[a]	2	4	14	30[d]	5

[a] *Was not tested for higher doses*
[b] *No preheating was applied*
[c] *Preheating at 175°C for 10 s*
[d] *Signal loss registered after 120 days of storage*

Conclusions

Based on the multiple analyses regarding the luminescence dosimetric properties of the vitroceramic and glass systems studied in the thesis and their potential applications in radiation dosimetry, the following main conclusions can be drawn:

- the best dosimetric properties of all Gd_2O_3 containing vitroceramic and glass systems are obtained for the $7Y_2O_3 \cdot 19Al_2O_3 \cdot 64SiO_2:10Gd_2O_3$ glass system that could be successfully employed for high-dose dosimetry using both TL and OSL techniques; it also has potential for medical dosimetry, for radiotherapy measurements and real-time monitoring of the actual dose delivered to the patient;
- it is not suitable for radiation dosimetry purposes the Gd_2O_3 doped $40SiO_2 \cdot 59.5B_2O_3:0.5Gd_2O_3$ borosilicate vitroceramic due to the low temperature TL peak;
- the Gd_2O_3 free $30P_2O_5 \cdot 40SiO_2:30Y_2O_3$ yttrium-phosphosilicate vitroceramic has potential for dose determinations in fractionated teletherapy and mixed neutron-gamma fields using the TL technique.

References

Akselrod, M.S., Bøtter-Jensen, L., McKeever, S.W.S., 2007. Optically stimulated luminescence and its use in medical dosimetry. Radiation Measurements 41, 78-99.

Alajerami, Y.S.M., Hashim, S., Ghoshal, S.K., Saleh, M.A., Kadni, T., Saripan, M.I., Alzimami, K., Ibrahim, Z., Bradley, D.A., 2013. The effect of TiO_2 and MgO on the thermoluminescence properties of a lithium potassium borate glass system. Journal of Physics and Chemistry of Solids 74, 1816-1822.

Azorin, J., 2014. Preparation methods of thermoluminescent materials for dosimetric applications: An overview. Applied Radiation and Isotopes 83, 187-191.

Banerjee, D., Bøtter-Jensen, L., Murray, A.S., 2000. Retrospective dosimetry: estimation of the dose to quartz using the single-aliquot regenerative-dose protocol. Applied Radiation and Isotopes 52, 831-844.

Barve, R.A., Suriyamurthy, N., Panigrahi, B.S., Venkatraman, B., 2015. Dosimetric investigations of Tb^{3+}-doped strontium silicate phosphor. Radiation Protection Dosimetry 163, 430-438.

Biró, B., Fenyvesi, A., Timar-Gabor, A., Simon, V., 2018. Thermoluminescence properties of $30Y_2O_3 \cdot 30P_2O_5 \cdot 40SiO_2$ vitroceramics in mixed neutron-gamma fields. Applied Radiation and Isotopes 135, 224-231.

Biró, B., Pascu, A., Timar-Gabor, A., Simon, V., 2015. Thermoluminescence investigations on $xY_2O_3 \cdot (60\text{-}x)P_2O_5 \cdot 40SiO_2$ vitroceramics. Applied Radiation and Isotopes 98, 49-53.

Bos, A.J.J., 2001. High sensitivity thermoluminescence dosimetry. Nuclear Instruments and Methods in Physics Research B 184, 3-28.

Bøtter-Jensen, L., McKeever, S.W.S., Wintle, A.G., 2003. Optically stimulated luminescence dosimetry. Elsevier, Amsterdam, 374 p.

Chrstie, J.K., Malik, J., Tilocca, A., 2011. Bioactive glasses as potential radioisotope vectors for in situ cancer therapy: investigating the structural effects of yttrium. Physical Chemistry Chemical Physics 13, 17749-17755.

Clark, R.A., Robertson, J.D., Schwantes, J.M., 2013. Intrinsic dosimetry: elemental composition effects on the thermoluminescence of commercial borosilicate glass. Radiation Measurements 59, 170-276.

Erbe, E.M., Day, D.E., 1993. Chemical durability of Y_2O_3-Al_2O_3-SiO_2 glasses for the in vivo delivery of beta radiation. Journal of Biomedical Materials Research 27, 1301–1308.

Fu, Y., Chrstie, J.K., 2017. Atomic structure and dissolution properties of yttrium containing phosphate glasses. International Journal of Applied Glass Science 8, 412-417.

Furetta, C., Prokić, M., Salamon, R., Prokić, V., Kitis, G., 2001. Dosimetric characteristics of tissue equivalent thermoluminescent TL solid TL detectors based on lithium borate. Nuclear Instruments and Methods in Physics Research A 456, 411-417.

Furetta, C., Weng, W., 1998. Operational thermoluminescence dosimetry. World Scientific Publishing, 252 p.

Inrig, E.L., Godfrey-Smith, D.I., Khana, S., 2008. Optically stimulated luminescence of electronic components for forensic, retrospective, and accident dosimetry. Radiation Measurements 43, 726-730.

Kadari, A., Pascu, A., Timar-Gabor, A., Simon, V., Kadri, D., 2016. Trapping parameters determination and modeling of the thermoluminescence process in SiO_2-P_2O_5 vitroceramics doped with different Y_2O_3 concentrations. Optik 127, 6162-6171.

Kortov, V., 2007. Materials for thermoluminescent dosimetry: current status and future trends. Radiation Measurements 42, 576–581.

Kortov, V., 2014. Modern trends and development in high-dose luminescent measurements. Journal of Physics: Conference Series 552, 012039.

Kortov, V., Ustyantsev, Yu., 2013. Advantages and challenges of high-dose thermoluminescent detectors. Radiation Measurements 56, 299-302.

Laopaiboon, R. and Bootjomchai, C., 2015. Thermoluminescence studies on alkali-silicate glass doped with dysprosium oxide for use in radiation dosimetry. Journal of Luminescence 158, 275-280.

Li, H., Su, Y., Li, L., Strachan, D.M, 2001. Raman spectroscopic study of gadolinium (III) in sodium-aluminoborosilicate glasses. Journal of Non-Crystalline Solids 292, 167-176.

Mayneord, W.V., 1937. The significance of the Roentgen. Acta of the International Union against Cancer 2, 271-282.

McKeever, S.W.S., Moscovitch, M., 2003. Topics under debate. On the advantages and disadvantages of optically stimulated luminescence dosimetry and thermoluminescence dosimetry. Radiation Protection Dosimetry 104, 263-270.

McKeever, S.W.S., Moscovitch, M., Townsend, P.D., 1995. Thermoluminescence dosimetry materials: properties and uses. Nuclear Technology Publishing, 210 p.

Murray, A.S., Roberts, R.G., Wintle, A.G., 1997. Equivalent dose measurement using a single aliquot of quartz. Radiation Measurements 27, 171-184.

Oliveira, L.C., Yukihara, E.G., Baffa, O., 2016. MgO:Li,Ce,Sm as a high-sensitivity material for optically stimulated luminescence dosimetry. Scientific Reports 6: 24348

Olko, P., 2010. Advantages and disadvantages of luminescence dosimetry. Radiation Measurements 45, 506-511.

Park, J., Lakes, R.S., 2007. Biomaterials: An Introduction, 3rd edition. Springer, New York, 562 p.

Park, J.B., 1984. Biomaterials Science and Engineering. Plenum Press, New York, 459 p.

Pascu, A., Timar-Gabor, A., Kadari, A., Simon, V., 2017. Structure, thermoluminescence characteristics and kinetic parameters of gadolinium doped borosilicate vitroceramic system. Romanian Journal of Materials 47, 309-314.

Plodinec, M.J., 2000. Borosilicate glasses for nuclear waste immobilization. Glass Technology 41, 186–192.

Polyakova, I.G., 2000. Alkali borosilicate systems: Phase diagrams and properties of glasses. Physics and Chemistry of Glasses 41, 247-258.

Pradhan, A.S., Lee, J.I., Kim, J.L., 2008. Recent developments of optically stimulated luminescence materials and techniques for radiation dosimetry and clinical applications. Journal of Medical Physics 33, 85-99.

Soares, 2002. National and international standards and calibration of thermoluminescence dosimetry systems. Radiation Protection Dosimetry 101, 167-172.

Sommer, M., Henniger, J., 2006. Investigation of a BeO-based optically stimulated luminescence dosimeter. Radiation Protection Dosimetry 119, 394-397.

Yukihara, E.G., Andrade, A.B., Eller, S., 2016. BeO optically stimulated luminescence dosimetry using automated research readers. Radiation Measurements 94, 27-34.

Yukihara, E.G., McKeever, S.W.S., Akselrod, M.S., 2014. State of art: optically stimulated luminescence dosimetry – frontiers and future research. Radiation Measurements 71, 15-24.

Yukihara, E.G., Milliken, E.D., Oliveira, L.C., Orante-Barrón, V.R., Jacobsohn, L.G., Blair, M.W., 2013. Systematic development of new thermoluminescence and optically stimulated luminescence materials. Journal of Luminescence 133, 203-210.

Yukihara, E.G., Mittani, J.C., Vanhavere, F., Akselrod, M.S., 2008. Development of new optically stimulated luminescence (OSL) neutron dosimeters. Radiation Measurements 43, 309-314.

Yusoff, A.L., Hugtenburg, R.P., Bradley, D.A, 2005. Review of development of a silica-based thermoluminescence dosimeter. Radiation Physics and Chemistry 74, 459-481.